

# CHEMISTRY

## A European Journal

A Journal of



### Accepted Article

**Title:** Free-standing metal oxide nanoparticle superlattices constructed with engineered protein containers show in crystallo catalytic activity

**Authors:** Tobias Beck, Marcel Lach, and Matthias Künzle

This manuscript has been accepted after peer review and appears as an Accepted Article online prior to editing, proofing, and formal publication of the final Version of Record (VoR). This work is currently citable by using the Digital Object Identifier (DOI) given below. The VoR will be published online in Early View as soon as possible and may be different to this Accepted Article as a result of editing. Readers should obtain the VoR from the journal website shown below when it is published to ensure accuracy of information. The authors are responsible for the content of this Accepted Article.

**To be cited as:** *Chem. Eur. J.* 10.1002/chem.201705061

**Link to VoR:** <http://dx.doi.org/10.1002/chem.201705061>

Supported by  
**ACES**

WILEY-VCH

# Free-standing metal oxide nanoparticle superlattices constructed with engineered protein containers show in crystallo catalytic activity

Marcel Lach, Matthias Künzle, and Tobias Beck\*

**Abstract:** The construction of defined nanostructured catalysts is challenging. In previous work, we established a strategy to assemble binary nanoparticle superlattices with oppositely charged protein containers as building blocks. Here, we show that these free-standing nanoparticle superlattices are catalytically active. The metal oxide nanoparticles inside the protein scaffold are accessible for a range of substrates and show oxidase-like and peroxidase-like activity. The stable superlattices can be reused for several reaction cycles. In contrast to bulk nanoparticle-based catalysts, which are prone to aggregation and difficult to characterize, nanoparticle superlattices based on engineered protein containers provide an innovative synthetic route to structurally defined heterogeneous catalysts with control over nanoparticle size and compositions.

For the application of nanostructured materials in catalysis, optics, electronics and sensor technology, a fine control over material composition and morphology is required because of the strong interplay between functionality and material structure.<sup>[1]</sup> This holds particularly true for catalysis, where access to the catalytically active surface is mandatory and a defined morphology and composition is required for reaction control. However, it remains difficult to construct well-defined nanomaterials, with precise distances between particles and sufficient reaction space around them. Towards this end, bottom-up approaches offer a solution. Here, nanoscale building blocks such as nanoparticles are assembled into three-dimensional materials with defined composition. Generally, organic ligands or DNA linkers are used to construct nanoparticle superlattices with diverse crystal symmetry, lattice parameters and compositions.<sup>[2]</sup> However, certain drawbacks exist. For nanoparticle assembly, the aforementioned approaches require ligands that block the access to the nanoparticles for catalysis, thus passivate the surface. This could explain why there have been a number of reports on the synthesis of nanoparticle superlattices,<sup>[2-3]</sup> but only a few studies on their catalytic properties have been published, necessitating the removal of the ligand scaffold by thermal decomposition.<sup>[4]</sup> Moreover, nanoparticle superlattices based on DNA linkers show only limited stability, which can be improved by elaborate post-processing.<sup>[4c]</sup>

[\*] Marcel Lach, Matthias Künzle, Dr. Tobias Beck  
RWTH Aachen University, Institute of Inorganic Chemistry;  
JARA-SOFT (Researching Soft Matter); and I3TM  
52074 Aachen (Germany)  
E-mail: [tobias.beck@ac.rwth-aachen.de](mailto:tobias.beck@ac.rwth-aachen.de)

Supporting information for this article is given via a link at the end of the document.

Protein scaffolds for nanoparticle superlattice assembly offer an alternative route to catalytically active and well-defined nanoparticle-based catalysts. Proteins can be assembled with atomic precision into highly structured materials, either on surfaces to form 2D films,<sup>[5]</sup> or as free-standing 3D crystals.<sup>[6]</sup> Furthermore, the protein scaffold can be readily stabilized by cross-linking of the building blocks in the protein crystals.<sup>[7]</sup> Importantly, protein crystals show a high solvent content, thus a high porosity, which enables 'in crystallo' enzymatic reactions,<sup>[8]</sup> soaking of heavy-metal compounds for protein structure determination,<sup>[9]</sup> or co-crystallization with insoluble dyes to produce singlet oxygen.<sup>[10]</sup> In this work, we use protein containers as building blocks to construct catalytically active nanoparticle superlattices based on protein crystals. The pores inherent to the protein containers and the channels inside the protein crystal enable access to the nanoparticles, thus overcoming previous challenges such as surface accessibility in nanoparticle-based catalysts. Moreover, for the first time, large-scale nanoparticle superlattices with dimensions up to several hundred micrometers were prepared and utilized in catalysis.

We have recently established engineered ferritin containers as building blocks for the construction of highly ordered binary nanoparticle superlattices.<sup>[11]</sup> In the first step, the protein containers are equipped with a number of charged amino acids on the outer surface,<sup>[12]</sup> to effort two oppositely charged protein containers.<sup>[11]</sup> Subsequently, metal oxide nanoparticle synthesis inside these engineered containers, which have an inner diameter of 7 nm and outer diameter of 12 nm, can be readily carried out by exploiting the container pores (Fig. 1A). For this work, we synthesized cerium oxide and iron oxide nanoparticles inside the engineered protein containers. In the final step, these nanoparticle-protein composites are used for the construction of binary nanoparticle superlattices (Fig. 1B).

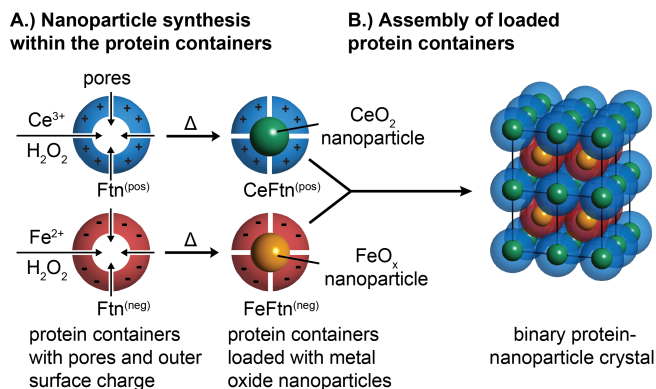


**Figure 1.** Strategy for the construction of binary metal oxide nanoparticle superlattices. A) Nanoparticle synthesis inside the ferritin container cavity, utilizing the container pores. B) Assembly of the nanoparticle-protein composites to form highly ordered binary nanoparticle superlattices.

For the current study, we mainly focused on cerium oxide nanoparticles, which have over the years found application in catalytic converters, solid oxide fuels cells, ultraviolet absorbers and oxygen sensors.<sup>[13]</sup> Recently, cerium oxide nanoparticles, also referred to as nanoceria, have been shown to have catalytic properties similar to enzymes.<sup>[14]</sup> Due to its high biocompatibility, nanoceria has been discussed as enzyme surrogate.<sup>[15]</sup> In general, nanoparticles can be superior to enzymes in terms of thermal stability and resistance against degradation. Moreover, catalytic nanoparticles can introduce orthogonal reactivity, not found in natural enzymatic reactions.<sup>[16]</sup> Therefore, the construction of multifunctional nanoparticle catalysts could produce materials with unparalleled catalytic activity and diversity.

As catalyst, cerium oxide nanoparticles were synthesized inside the positively charged ferritin container  $\text{Ftn}^{(\text{pos})}$  and the negatively charged container  $\text{Ftn}^{(\text{neg})}$  (see supporting information for procedures) to yield  $\text{CeFtn}^{(\text{pos})}$  and  $\text{CeFtn}^{(\text{neg})}$ . Powder X-ray diffraction shows that the particles inside the containers are  $\text{CeO}_2$ , with the same crystal structure as commercially available  $\text{CeO}_2$  nanoparticles (Fig. S1). The engineered protein containers serve a threefold purpose: a) The ferritin containers are a reaction template: The inner protein container cavity provides a size-constraining vessel for the synthesis of nanoparticles, as shown in several examples.<sup>[17]</sup> Moreover, protein containers with encapsulated nanoparticles or enzymes have been applied for a number of catalytic conversions.<sup>[18]</sup> b) The engineered ferritin containers have a charged outer surface, which enables assembly of binary nanoparticles lattices<sup>[11]</sup> (Fig. 1), for the construction of multifunctional materials. c) The containers' inherent pores enable *in situ* synthesis of nanoparticles inside the cavity. Importantly, after formation of the container-nanoparticle composite, these pores provide access to the nanoparticles for catalytic turnover. Although a number of protein container-nanoparticle composites have been synthesized,<sup>[17]</sup> only very few catalytic systems have been kinetically characterized in solution.<sup>[17e, 17f]</sup> Therefore, we investigated the reactivity of the container-nanoparticle composite both in solution and in the nanoparticle superlattice.

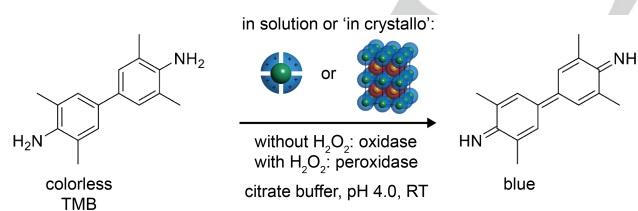


**Figure 2.** Catalytic oxidation of 3,3',5,5'-tetramethylbenzidine (TMB) in solution and in the nanoparticle superlattice using encapsulated cerium oxide nanoparticles to form the oxidized substrate with blue color.

3,3',5,5'-tetramethylbenzidine (TMB), a substrate for horseradish peroxidase commonly used in bioassays,<sup>[19]</sup> was used to investigate the catalytic oxidation to the readily traceable blue oxidation product (Fig. 2). The reaction was started by mixing catalyst, either  $\text{CeFtn}^{(\text{pos})}$  or  $\text{CeFtn}^{(\text{neg})}$ , with the TMB substrate. Reactions with TMB under aerobic atmosphere were conducted

to investigate the oxidase-like activity, with oxygen as the oxidant. For peroxidase-like activity, hydrogen peroxide was added to the reaction mixture. Cerium oxide nanoparticles do not show any strong absorption in the visible range, preventing any spectral overlap with the dye molecule. The reaction was followed by monitoring the absorbance maximum of the oxidized TMB at 645 nm. Reaction without hydrogen peroxide shows a turnover to the blue colored product within hours (Fig. 3A and B), which is also observed in the corresponding UV-Vis spectra for  $\text{CeFtn}^{(\text{pos})}$  and  $\text{CeFtn}^{(\text{neg})}$  (Fig. 3C). No background reaction was observed without catalyst. Peroxidase-like activity in the presence of hydrogen peroxide proceeds at a faster rate: the blue color is visible within minutes (Fig. 3D).

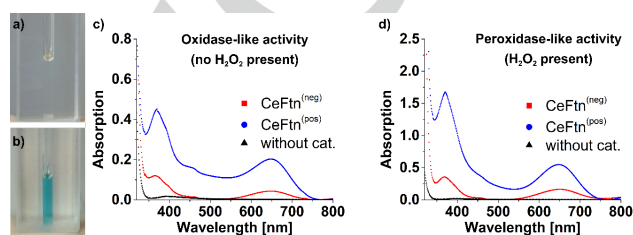


**Figure 3.** Catalysis in solution. Solution with 1 mM TMB and catalyst at 0 min (a) and after one day (b). Absorption spectra of TMB after catalytic reaction with  $\text{CeO}_2$  in  $\text{Ftn}^{(\text{pos})}$  and  $\text{Ftn}^{(\text{neg})}$ : oxidase-like activity after 1 day (c) and peroxidase-like activity with hydrogen peroxide present. Incubation time 15 min (d).

Kinetic parameters for the oxidase-like and peroxidase-like activity of  $\text{CeFtn}^{(\text{pos})}$  and  $\text{CeFtn}^{(\text{neg})}$  in solution were determined by varying the concentrations of TMB and hydrogen peroxide (see supporting information for details, Figs. S2 and S3), and are shown in Tab. 1.

**Table 1.** Comparison of the kinetic parameters for oxidase-like (no  $\text{H}_2\text{O}_2$ ) or peroxidase-like activity (with  $\text{H}_2\text{O}_2$ ) using the cerium nanoparticles synthesized within the two protein containers,  $\text{CeFtn}$ .

Building block	Substrate	$v_{\text{max}}$ [ $\mu\text{M s}^{-1}$ ]	$K_m$ [mM]
$\text{CeFtn}^{(\text{pos})}$	TMB	$2.2 \times 10^{-3}$	1.54
$\text{CeFtn}^{(\text{pos})}$	TMB + $\text{H}_2\text{O}_2$	$1.2 \times 10^{-2}$	15.39
$\text{CeFtn}^{(\text{neg})}$	TMB	$7.3 \times 10^{-4}$	0.83
$\text{CeFtn}^{(\text{neg})}$	TMB + $\text{H}_2\text{O}_2$	$3.3 \times 10^{-3}$	4.05

For  $\text{CeFtn}^{(\text{pos})}$  a higher activity is observed compared to  $\text{CeFtn}^{(\text{neg})}$ . This difference can be attributed to the fact that the nanoparticle loading is higher for  $\text{CeFtn}^{(\text{pos})}$ : After the sucrose gradient centrifugation, the peak for the maximum absorption at 322 nm in the  $\text{CeFtn}^{(\text{pos})}$  sample is found at a higher fraction number compared to  $\text{CeFtn}^{(\text{neg})}$  (Fig. S4). This shift indicates that the  $\text{CeO}_2$  nanoparticles for  $\text{Ftn}^{(\text{pos})}$  have a higher mass and thus  $\text{Ftn}^{(\text{pos})}$  has a higher loading efficiency compared with  $\text{Ftn}^{(\text{neg})}$ . The higher loading efficiency in the final samples (same protein concentration) can also be observed with UV-Vis absorption spectroscopy (Fig. S5).<sup>[11]</sup> Previous syntheses of the cerium

oxide nanoparticles also showed using transmission electron microscopy that CeFtn<sup>(pos)</sup> yielded slightly larger nanoparticles.<sup>[11]</sup> Notably, the reaction velocity in the presence of hydrogen peroxide (peroxidase-like activity) is faster for CeFtn<sup>(pos)</sup> and CeFtn<sup>(neg)</sup> each, possibly due to different reaction pathways. For peroxidase-like activity, the cerium oxide nanoparticles likely catalyze a Fenton-like reaction,<sup>[14, 20]</sup> with conversion of hydrogen peroxide to hydroxyl and superoxide radicals that readily diffuse out of the container and react with the substrate. For the oxidase-like activity (no hydrogen peroxide present), the substrate needs to diffuse into the container to be oxidized on the particle's surface. A similar trend in reaction velocity and  $K_m$  with and without hydrogen peroxide was observed for ferritin loaded with platinum nanoparticles.<sup>[17f]</sup> Comparing the kinetic parameters for CeFtn composites with cerium oxide nanoparticles coated with polymer ligands<sup>[21]</sup> shows that the oxidase-like reaction velocity for the protein-nanoparticle composites is considerable slower (factor  $10^3$ ), because the substrates need to diffuse through the container pores into the cavity for turnover, and out after the reaction. Interestingly, the Michaelis constants are rather similar compared to polymer-coated nanoparticles, indicating a similar binding affinity to the nanoparticle surface for both types of catalysts.<sup>[21]</sup> We also characterized the activity of the negatively charged container loaded with iron oxide nanoparticles, FeFtn<sup>(neg)</sup>, towards catalytic oxidation of TMB. As expected, these protein-nanoparticle composites do not show any oxidase-like activity. In contrast to CeFtn, additional hydrogen peroxide is required for the oxidation of TMB with FeFtn<sup>(neg)</sup> (Figs. S6 and S7). Kinetic parameters are shown in Tab. S1 and show a similar reaction rate compared with CeFtn<sup>(pos)</sup> and CeFtn<sup>(neg)</sup>.

We were particularly interested if the catalytic activity observed in solution is preserved within the nanoparticle superlattices. With the oppositely charged protein containers as building blocks, nanoparticles were assembled (Fig. 1B) to yield crystalline samples with dimensions up to several hundred micrometers (Fig. S8), using crystallization conditions previously established.<sup>[11]</sup> Before the materials were subjected to catalytic investigations, the protein scaffold was stabilized by incubation with a dialdehyde that cross-links the side chains inside the crystals. The nanoparticle crystals prepared in this way can be readily manipulated. Moreover, they are stable in reaction solutions for testing catalytic activity. As first samples, we used nanoparticle superlattices with cerium oxide nanoparticles. Either Ftn<sup>(pos)</sup> or Ftn<sup>(neg)</sup>, or both containers are filled with nanoparticles and assembled into highly ordered superlattices. Importantly, incubation of the crystalline materials with a solution containing TMB shows that the cerium oxide nanoparticles are catalytically active within the protein matrix and show a deep coloration within minutes for the CeFtn<sup>(pos)</sup> / CeFtn<sup>(neg)</sup> crystals (Fig. 4A, C, E). This can also be observed for crystals with either container filled with CeO<sub>2</sub> (Fig. S9). Peroxidase activity is also observed for all three nanoparticle superlattices (Fig. S10). The crystal concentrates the catalytically active nanoparticles in a confined space. Therefore, the turnover is more quickly visible in the nanoparticle superlattice compared to solution. After the reaction, the converted substrate can diffuse out of the crystal.

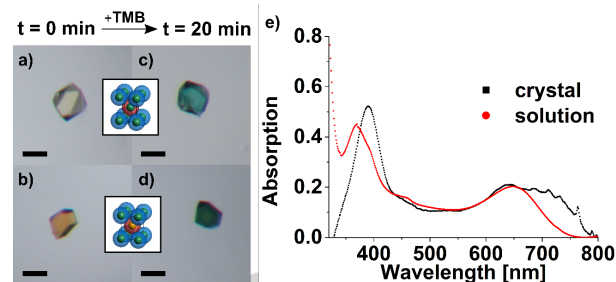


**Figure 4.** a) CeFtn<sup>(pos)</sup> / CeFtn<sup>(neg)</sup> crystals b) CeFtn<sup>(pos)</sup> / CeFtn<sup>(neg)</sup> crystal after 20 minutes incubation with TMB substrate c) CeFtn<sup>(pos)</sup> / FeFtn<sup>(neg)</sup> crystal after 20 minutes incubation with TMB substrate d) CeFtn<sup>(pos)</sup> / FeFtn<sup>(neg)</sup> crystal after 20 minutes incubation with TMB substrate. Scale bar is 100  $\mu$ m. e) UV-Vis absorption spectrum of a CeFtn<sup>(pos)</sup> / CeFtn<sup>(neg)</sup> crystal cut into thin slices.

Further investigations on in crystallo activity were carried out with nanoparticle superlattices constructed with iron oxide nanoparticles, FeFtn<sup>(neg)</sup>. Incubation with TMB under aerobic atmosphere did not show any reaction, thus no oxidase-like activity (Fig. S11A), which is in accordance with the experiments with the protein-nanoparticle composites in solution (see above). Incubation of the iron oxide nanoparticle superlattice with TMB in presence of H<sub>2</sub>O<sub>2</sub> showed oxidation to the colored product, thus peroxidase activity (Fig. S11B), as observed in solution.

As a step towards multifunctional materials, we constructed nanoparticle superlattices with cerium and iron oxide nanoparticles. These binary superlattices showed as expected oxidase-like activity due to the cerium oxide nanoparticles (Fig. 4B and D). The iron oxide nanoparticles do not hamper the activity of the cerium oxide nanoparticles. Here, a synergistic effect is not present, because only CeFtn shows oxidase activity whereas FeFtn does not (see also Fig. 3). The combination of two different nanoparticles in the protein scaffold does not influence the activity of the single nanoparticle type. A more detailed analysis of the kinetic parameters requires a larger amount of materials, which will be produced using batch crystallization techniques. Importantly, by measuring the product concentration in the supernatant, we could show that the crystalline samples are stable and enable several cycles of catalytic turnover with high activity remaining in each cycle (Fig. S12). Moreover, this is an advancement compared to previous reports on catalytically active nanoparticle superlattices.<sup>[4c]</sup> In the protein scaffold, the nanoparticles are not passivated nor is the particle superlattice inactivated by the substrates.

To investigate the substrate scope of the oxidation reaction, several dyes with different size were tested for conversion with CeFtn<sup>(pos)</sup> / CeFtn<sup>(neg)</sup> crystals as catalyst without hydrogen peroxide present (see supporting information for details). Here, FeFtn crystals were not used due to the strong color of iron oxide nanoparticle crystals. The dye molecules are readily converted inside the nanoparticle superlattice as evidenced by deep coloration of the crystals incubated with substrate solution (Fig. S13-S17). Interestingly, the substrates are slightly larger in thickness than the container pore size at the three-fold channel (TMB 5 Å vs. pore 4 Å, Fig. S18). Obviously, the flexibility of the ferritin pores, observed already for incorporation of large molecules such as organometallic complexes into the ferritin cavity,<sup>[22]</sup> enables the substrates accessing the nanoparticles. By

comparing the reaction rate of the substrates to the reaction rate of TMB in the crystals, it can be concluded that 3,3'-diaminobenzidine and 3-amino-9-ethylcarbazole (Fig. S16 and S17) show a similar reaction rate as TMB, as coloration of the crystals is observed within minutes. O-phenyldiamine, 5-aminosalicylic acid and o-dianisidine react considerably slower (Fig. S13 – S15), because coloration is only clearly visible after one day. Because there is no correlation of substrate size and reactivity, the reactivity does apparently not depend on the size of the substrates used in this study. Nevertheless, the container pores and the crystal channels (diameter of about 10 Å, Fig. S19) could offer a potential filter effect, e.g. with regard to the size or polarity of the substrates, further exploited by engineering the containers' pores and crystal lattice channels.

Our results demonstrate that engineered protein containers can function as building blocks for well-defined heterogeneous catalysts based on metal oxide nanoparticles. The nanoparticles show oxidase-like and peroxidase-like activity inside the crystalline material. The nanoparticle materials are stable in solution and can be produced with lateral dimensions up to several hundred micrometers. The protein scaffold provides stability to the nanoparticles but ensures access to the nanoparticles via the channels within the crystal and the protein container pores. In this way, a long-standing challenge, nanoparticle surface accessibility in nanoparticle superlattices, is overcome. In addition to providing stability to the nanoparticle lattice, the protein scaffold can also impart biocompatibility of the material, important for applications in the biomedical field. Here, the utilization of nanoparticles is still hampered by their compatibility and stability in biological systems. The presented binary system enables a fine control over the composition of the heterogeneous catalyst. Along these lines, binary superlattices built from nanoparticles, also other than the ones used in the current study, with different or complementary catalytic functionality could catalyze cascade reactions within the protein scaffold.

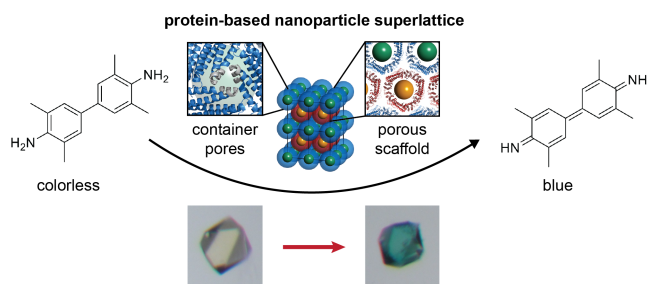
## Acknowledgements

We thank Prof. Ulrich Schwaneberg for generous support with regard to protein production and Prof. Ulrich Simon for general support and helpful discussions. This work was generously supported by a Liebig scholarship to T.B. (Fonds der Chemischen Industrie), a doctoral scholarship to M.L. (Cusanuswerk), a doctoral scholarship to M.K. (Fonds der Chemischen Industrie), and the Excellence Initiative of the German federal and state governments (I3TM Seed Fund grant and I3TM Step2Project grant to T.B.).

**Keywords:** protein engineering • protein container • nanocatalysis • nanoparticles • nanoparticle superlattice

- [1] a) D. V. Talapin, J.-S. Lee, M. V. Kovalenko, E. V. Shevchenko, *Chem. Rev.* **2010**, *110*, 389-458; b) A.-H. Lu, W. Schmidt, N. Matussevitich, H. Bönemann, B. Spliethoff, B. Tesche, E. Bill, W. Kiefer, F. Schüth, *Angew. Chem. Int. Ed.* **2004**, *43*, 4303-4306; c) L. Jiang, Y. Sun, F. Huo, H. Zhang, L. Qin, S. Li, X. Chen, *Nanoscale* **2012**, *4*, 66-75; d) V. F. Puentes, P. Gorostiza, D. M. Arugnete, N. G. Bastus, a. P. Alivisatos, *Nat. Mater.* **2004**, *3*, 263-268; e) A. K. Gupta, M. Gupta, *Biomaterials* **2005**, *26*, 3995-4021.
- [2] a) E. V. Shevchenko, D. V. Talapin, N. A. Kotov, S. O'Brien, C. B. Murray, *Nature* **2006**, *439*, 55-59; b) X. Ye, J. Chen, C. B. Murray, *J. Am. Chem. Soc.* **2011**, *133*, 2613-2620; c) R. J. Macfarlane, M. R. Jones, B. Lee, E. Auyeung, C. A. Mirkin, *Science* **2013**, *341*, 1222-1225; d) C. Zhang, R. J. Macfarlane, K. L. Young, C. H. J. Choi, L. Hao, E. Auyeung, G. Liu, X. Zhou, C. A. Mirkin, *Nat. Mater.* **2013**, *12*, 741-746.
- [3] a) S. Y. Park, A. K. R. Lytton-Jean, B. Lee, S. Weigand, G. C. Schatz, C. Mirkin, *Nature* **2008**, *451*, 553-556; b) D. Nykpanchuk, M. M. Maye, D. van der Lelie, O. Gang, *Nature* **2008**, *451*, 549-552; c) M. A. Kostianen, P. Hiekkataipale, A. Laiho, V. Lemieux, J. Seitsonen, J. Ruokolainen, P. Ceci, *Nat. Nanotechnol.* **2013**, *8*, 52-56.
- [4] a) Y. Kang, X. Ye, J. Chen, L. Qi, R. E. Diaz, V. Doan-Nguyen, G. Xing, C. R. Kagan, J. Li, R. J. Gorte, et al., *J. Am. Chem. Soc.* **2013**, *135*, 1499-1505; b) J. Li, Y. Wang, T. Zhou, H. Zhang, X. Sun, J. Tang, L. Zhang, A. M. Al-Enizi, Z. Yang, G. Zheng, *J. Am. Chem. Soc.* **2015**, *137*, 14305-14312; c) E. Auyeung, W. Morris, J. E. Mondloch, J. T. Hupp, O. K. Farha, C. A. Mirkin, *J. Am. Chem. Soc.* **2015**, *137*, 1658-1662.
- [5] a) P. Ringler, *Science* **2003**, *302*, 106-109; b) S. Gonen, F. DiMaio, T. Gonen, D. Baker, *Science* **2015**, *348*, 1365-1368.
- [6] a) P. A. Sontz, J. B. Bailey, S. Ahn, F. A. Tezcan, *J. Am. Chem. Soc.* **2015**, *137*, 11598-11601; b) C. J. Lanci, C. M. Macdermaid, S.-g. Kang, R. Acharya, B. North, X. Yang, *Proc. Natl. Acad. Sci. U.S.A.* **2012**, *109*, 7304-7309.
- [7] J. J. Roy, T. E. Abraham, *Chem. Rev.* **2004**, *104*, 3705-3721.
- [8] a) A. Mozzarelli, G. L. Rossi, *Annu. Rev. Biophys. Biomol. Struct.* **1996**, *25*, 343-365; b) A. L. Margolin, M. A. Navia, *Angew. Chem. Int. Ed.* **2001**, *40*, 2204-2222.
- [9] a) T. Beck, A. Krasauskas, T. Gruene, G. M. Sheldrick, *Acta Crystallogr. Sect. D* **2008**, *64*, 1179-1182; b) A. C. W. Pike, E. F. Garman, T. Krojer, F. von Delft, E. P. Carpenter, *Acta Crystallogr. Sect. D* **2016**, *72*, 303-318.
- [10] J. Mikkilä, E. Anaya-Plaza, V. Liljeström, J. R. Caston, T. Torres, A. de la Escosura, M. A. Kostianen, *ACS Nano* **2016**, *10*, 1565-1571.
- [11] M. Künzle, T. Eckert, T. Beck, *J. Am. Chem. Soc.* **2016**, *138*, 12731-12734.
- [12] T. Beck, S. Tetter, M. Künzle, D. Hilvert, *Angew. Chem. Int. Ed.* **2015**, *54*, 937-940.
- [13] a) M. Lei, T. Z. Yang, W. J. Wang, K. Huang, R. Zhang, X. L. Fu, H. J. Yang, Y. G. Wang, W. H. Tang, *Int. J. Hydrogen Energy* **2013**, *38*, 205-211; b) M. Aguirre, M. Paulis, J. R. Leiza, *Journal of Materials Chemistry A* **2013**, *1*, 3155-3155; c) I. Shitanda, S. Mori, M. Itagaki, *Anal. Sci.* **2011**, *27*, 1049-1052; d) J. Kašpar, P. Fornasiero, N. Hickey, *Catal. Today* **2003**, *77*, 419-449.
- [14] C. Xu, X. Qu, *NPG Asia Mater.* **2014**, *6*, e90.
- [15] X. Liu, W. Wei, Q. Yuan, X. Zhang, N. Li, Y. Du, G. Ma, C. Yan, D. Ma, *Chem. Commun.* **2012**, *48*, 3155-3157.
- [16] L. L. Chng, N. Erathodiyil, J. Y. Ying, *Acc. Chem. Res.* **2013**, *46*, 1825-1837.
- [17] a) F. C. Meldrum, B. R. Heywood, S. Mann, *Science* **1992**, *257*, 522-523; b) R. M. Kramer, C. Li, D. C. Carter, M. O. Stone, R. R. Naik, *J. Am. Chem. Soc.* **2004**, *126*, 13282-13286; c) M. Uchida, M. L. Flenniken, M. Allen, D. A. Willits, B. E. Crowley, S. Brumfield, A. F. Willis, L. Jackiw, M. Jutila, M. J. Young, T. Douglas, *J. Am. Chem. Soc.* **2006**, *128*, 16626-16633; d) C. A. Butts, J. Swift, S.-G. Kang, L. Di Costanzo, D. W. Christianson, J. G. Saven, I. J. Dmochowski, *Biochemistry* **2008**, *47*, 12729-12739; e) Z. Varpness, J. W. Peters, M. Young, T. Douglas, *Nano Lett.* **2005**, *5*, 2306-2309; f) J. Fan, J.-J. Yin, B. Ning, X. Wu, Y. Hu, M. Ferrari, G. J. Anderson, J. Wei, Y. Zhao, G. Nie, *Biomaterials* **2011**, *32*, 1611-1618.
- [18] a) A. Liu, C. H. H. Traulsen, J. J. L. M. Cornelissen, *ACS Catalysis* **2016**, *6*, 3084-3091; b) A. Liu, L. Yang, C. H. H. Traulsen, J. J. L. M. Cornelissen, *Chem. Commun.* **2017**, *53*, 7632-7634; c) P. C. Jordan, D. P. Patterson, K. N. Saboda, E. J. Edwards, H. M. Miettinen, G. Basu, M. C. Thielges, T. Douglas, *Nature Chemistry* **2015**, *8*, 1-7; d) Y. Azuma, R. Zschoche, M. Tinzl, D. Hilvert, *Angew. Chem. Int. Ed.* **2016**, *55*, 1531-1534; e) S. Tetter, D. Hilvert, *Angew. Chem. Int. Ed.* **2017**, 10.1002/anie.201708530, 1-5.
- [19] A. Frey, B. Meckelein, D. Extermest, M. A. Schmidt, *J. Immunol. Methods* **2000**, *233*, 47-56.
- [20] E. G. Heckert, S. Seal, W. T. Self, *Environ. Sci. Technol.* **2008**, *42*, 5014-5019.
- [21] A. Asati, S. Santra, C. Kaittanis, S. Nath, J. M. Perez, *Angew. Chem. Int. Ed.* **2009**, *48*, 2308-2312.
- [22] a) S. Abe, K. Hirata, T. Ueno, K. Morino, N. Shimizu, M. Yamamoto, M. Takata, E. Yashima, Y. Watanabe, *J. Am. Chem. Soc.* **2009**, *131*, 6958-6960; b) S. Zhang, J. Zang, H. Chen, M. Li, C. Xu, G. Zhao, *Small* **2017**, *13*, 1701045-1701045.

## COMMUNICATION



**Nanoparticle superlattices for catalysis:** Engineered protein containers can assemble metal oxide nanoparticles into crystalline three-dimensional materials. The nanoparticles, which are accessible within the protein scaffold through the protein container pores and crystal channels, catalyze the conversion of a range of dye substrates.

Marcel Lach, Matthias Künzle, and Tobias Beck \*

Page No. – Page No.

**Free-standing metal oxide nanoparticle superlattices constructed with engineered protein containers show in crystallo catalytic activity**